Application of Second-Order Sliding Mode Concepts to Active Magnetic Bearings

Mohamed S. Kandil, *Student Member*, *IEEE*, Maxime R. Dubois, *Member*, *IEEE*, Loicq S. Bakay, and João P. Trovão, *Member*, *IEEE*

***Abstract*— Rotor mass imbalance is a common problem to rotating machines due to the unavoidable imperfections in manufacturing. These imbalance forces can be viewed as harmonic disturbances which lead to a periodic rotor runout during rotation. Furthermore, the runout length increases with the rotational speed squared. Moreover, for variable rotational speed applications, these harmonic disturbances are also time-varying. Active magnetic bearings (AMB) provide a mean to actively attenuate these disturbances. Although, various imbalance compensation schemes have been proposed in literature to handle this problem, they are often more suitable for constant rotational speed applications where disturbances can be handled at a predetermined rotational speed. This study proposes the application of second-order sliding mode control (2-SMC) to regulate AMB systems throughout a wide operating speed range. The proposed controllers are composed of two components. The first component is a linear controller for the sake of stabilizing the inherently unstable system, while the second component is a 2-SMC to handle the model uncertainties of the system as well as the exogenous harmonic disturbances. Simulation and experimental results are provided to demonstrate the effectiveness and superiority of the proposed techniques compared to the conventional linear controller.**

***Index Terms*— Active magnetic bearings (AMB), second-order sliding-mode control (2-SMC), time-varying harmonic disturbances, vibration control.**

I. Introduction

Rotating machines suffer from a common problem known as rotor mass imbalance which leads to vibrations in the rotor in the form of harmonic disturbances. As a result, centrifugal forces or imbalance forces are generated when the rotor rotates about its geometric axis and eventually yield the unpleasant rotor vibrations phenomenon. Unlike mechanical bearings, active magnetic bearings (AMB) have the capability of regulating rotor dynamics and achieving active vibration control via generating proper electromagnetic forces. Furthermore, the tremendous advantages of AMB include being lubricant-free, mechanically wear-free, and providing a frictionless support to rotating machines. Moreover, they have a longer life time, lower need to maintenance, and lower losses when compared to the conventional mechanical bearings. Over the past years, they have been applied in many industrial applications such as high-speed drive systems, energy storage flywheels, turbo-machinery [1].

In principle, the existing control schemes can be categorized into two groups, robust control and imbalance compensation schemes. For robust control approach, decentralized robust controllers [2] and more efficient (but more complicated as well) centralized control schemes [3] have been proposed in the literature. Gain-scheduled robust controllers have been investigated for variable rotational speed applications [4]. Recently, linear parameter varying (LPV) control approach has been proposed to eliminate the need for gain-scheduling which could lack to stability and/or performance guarantees [5]. However, this technique eventually yields extremely high order controllers. Subsequently, their real-time implementation is nontrivial and requires a very powerful control platform. For the imbalance compensation schemes, various approaches have been proposed such as adaptive vibration control (AVC) [6], and notch filters [7]. Although extending notch filter based schemes to a wide range of rotation is possible through gain scheduling the parameters of the notch filters, the successful implementation depends very much on the accuracy of speed measurement. For AVC, rotation throughout a wide speed range is also feasible. However, besides complex nonlinear adaptation mechanisms are often used, the convergence could not be guaranteed in all cases [8]. Moreover, the precise measurement of the rotation speed is necessary for the successful practical implementation.

Over the past years, sliding mode control (SMC) has gained a significant interest because of the claimed invariance to matched model uncertainties and external disturbances. It is the discontinuous control action that gives the interesting

Manuscript received October 30, 2016; revised March 09, and May 09 2017; accepted June 05, 2017. This work was supported in part by the Fonds de recherche du Québec – Nature et technologies, the Canada Research Chairs Program and the National Sciences and Engineering Research Council of Canada.

M. S. Kandil is with the e-TESC lab, the Department of Electrical Engineering, Université de Sherbrooke, Sherbrooke J1K 2R1, Canada, and also with the Department of Power Systems and Electric Machines, Zagazig University, Egypt (e-mail: Mohamed.Kandil@usherbrooke.ca).

M R. Dubois, and J. P. Trovão are with the Department of Electrical Engineering and Computer Engineering, Université de Sherbrooke, Canada (e-mail: Maxime.Dubois@usherbrooke.ca; Joao.Trovao@usherbrooke.ca).

L. Bakay is with GE Renewable Energy, Sorel-Tracy, Canada (e-mail: Loicq.Bakay@gmail.com).

features to this controller. Nevertheless, the practical implementation of an ideal SMC is not feasible because of the so-called chattering problem [9]–[11]. This drawback is non-acceptable in many applications such as mechanical systems due to the potential wear and tear of actuator and the possible loss of system stability. The commonly used solution in the conventional sliding mode control (CSMC) literature to handle chattering problem is the boundary layer approach [9]. This approach would effectively solve the problem but on the price of losing the complete invariance property. As a result, a compromise between the performance and the allowable chattering level is inevitable [11]. The principles of CSMC have been investigated and experimentally tested for compensating harmonic disturbances in AMB, e.g. [12], [13]. Some efforts have also been made to enhance the performance of these CSMC, such as incorporating a disturbance observer [14], or via adaptive control and neural networks [15]. However, the performance of these control techniques was validated at a constant rotational speed only. Few efforts have been made to investigate the performance of SMC principles to confront the time-varying harmonic disturbances in the case of a wide speed range. In [16], a gain-scheduled sliding manifold was proposed. However, it was observed that the performance degraded at the critical speeds. In [17], the sliding manifold was designed using μ-synthesis technique. Although it was claimed that the performance was satisfactory, the performance of that algorithm was not compared against any other control technique.

As an alternative approach, higher order sliding modes (HOSM) have been developed for handling the chattering problem while maintaining the main advantages of the CSMC with respect to robustness, order reduction, simplicity and ease of implementation [18]. Furthermore, the practical implementation of HOSM results in a higher accuracy compared to the CSMC in the presence of switching delays and measurement noise [19]. The competence of HOSM has been demonstrated in different applications [20]–[25]. Recently, this promising technique has been considered for AMB application. In [26], a decentralized control scheme based on a modified super twisting 2-SMC algorithm was proposed. In [27], a new multivariable continuous 2-SMC algorithm was designed. A centralized scheme was proposed for controlling a five degrees of freedom AMB system (one thrust bearing and two radial bearings). However, the performance of both the decentralized scheme in [26] and the centralized scheme in [27] were proposed for constant speed AMB applications. Furthermore, their performances were demonstrated via simulation results only with no comparison against any other control scheme. In literature, some 2-SMC contributions have also been reported for single degree of freedom AMB systems (e.g. thrust AMB and MAGLEV systems) [28]–[30]. However, the control problem in these systems is simple compared to the radial AMB. Furthermore, they do not suffer from any harmonic disturbances since no rotation is involved.

This paper proposes the application of two popular second-order sliding mode control (2-SMC) techniques, namely the twisting and the suboptimal algorithms, to regulate the operation of AMB systems in a wide operating speed range. The proposed control schemes are composed of two parts. The first one is a linear proportional-integral-derivative controller (PID) for the sake of stabilizing the inherently unstable system, while the second part is the 2-SMC which is devoted to handle the model uncertainties of the system as well as the exogenous time-varying harmonic disturbances. To the best of our knowledge, this is the first experimental study to report the application of 2-SMC techniques to handle time-varying harmonic disturbances in multi-axis AMB. The novelty and contributions of this study compared to the existing methods can be summarized as follows: (i) The concept of proposing 2-SMC algorithms as an add-on to enhance the disturbance attenuation performance of the PID control (the widely-adopted controller for industrial applications). (ii) Addressing the application of both twisting and suboptimal 2-SMC algorithms for variable rotational speed AMB applications. (iii) The experimental implementation of these algorithms on a practical control platform. (iv) Conducting a fair comparative analysis between a well-tuned PID controller and the same one but equipped with the proposed 2-SMC add-ons. (v) Deriving a condition that shows the bandwidth limitation of 2-SMC approach with respect to the effective handling of harmonic disturbances, see Appendix II.

This paper is organized as follows. In Section II, the mathematical model for rotor-AMB with rotor mass imbalance is presented. Sections III presents the second-order sliding mode control principles. Section IV presents the proposed control schemes. Section V is devoted to presenting simulation results and experimental validation. Finally, Section VI concludes this paper.

II. Mathematical Model

A. Rotor-AMB Model

The mechanical diagram for the rotor-bearing system is illustrated in Fig. 1. The rotor is assumed to be rigid. Following Newton–Euler equations, the dynamic behavior for this system about the center of gravity (COG) can be described as follows [1]:

$$\begin{cases} m\,\ddot{x}_s = F_{x1} + F_{x2} + f_{dx} \\ m\,\ddot{y}_s = F_{y1} + F_{y2} - m\,g + f_{dy} \\ J_r\,\ddot{\theta}_y - J_z\omega\,\dot{\theta}_x = -l_1 F_{x1} + l_2 F_{x2} \\ J_r\,\ddot{\theta}_x + J_z\omega\,\dot{\theta}_y = l_1 F_{y1} - l_2 F_{y2} \end{cases} \tag{1}$$

where x_s and y_s represent the displacement of the rotor with respect to the COG while θ_x and θ_y denote the angular displacement of the rotor around the x and y axes respectively; m denotes the rotor mass, J_r and J_z are the rotor transverse and polar moments of inertia respectively; ω is the rotational speed of the rotor; F_{x1}, F_{y1}, F_{x2}, and F_{y2}, are the resultant horizontal and vertical forces at the first and second radial bearings B_1, B_2 respectively; f_{dx} and f_{dy} are the external disturbances acting on

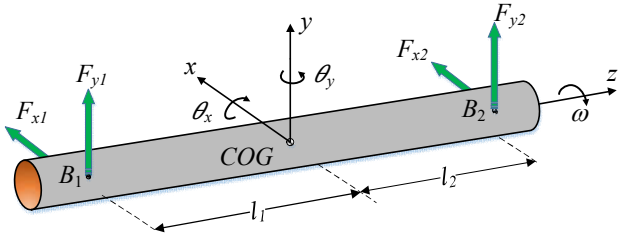

Fig. 1. Mechanical diagram for the rotor-bearing system.

the rotor; and lengths l_1 and l_2 are the distance between the first and second bearings and the COG respectively.

The electromagnetic forces in (1) are typically nonlinear functions in terms of coil currents and rotor displacements. Taylor expansion is usually applied for achieving linearization around the geometric center of the bearing. For instance, let us consider the electromagnetic forces of bearing B_1, the linearized bearing forces, F_{x1} and F_{y1} acting along the x- axis and y- axis directions respectively can be written as follows:

$$\begin{aligned} F_{x1} &\cong 0 + k_{sx}\, x_1 + k_{ix}\, i_{x1} \\ F_{y1} &\cong F_{y10} + k_{sy}\, y_1 + k_{iy}\, i_{y1} \end{aligned} \tag{2}$$

where F_{y10} represents the constant force component generated by the biasing current I_{y1} compensate the static load acting on bearing B_1 which usually equals to half of the rotor weight, x_1 and y_1 represent the horizontal and vertical deviations respectively, i_{x1} and i_{y1} are the control currents for horizontal and vertical axes respectively, while the parameters k_{sx}, k_{sy}, k_{ix}, and k_{iy} are defined in Table II, see Appendix I. The forces generated at bearing B_2 can be formulated in a similar manner to (2).

B. External Disturbances

Rotor mass imbalance forces are the major source for external harmonic disturbances which can be represented by two perpendicular components f_{dx} and f_{dy} acting on the horizontal and vertical axes respectively. The imbalance forces can be modeled as [8]:

$$\begin{aligned} f_{dx} &= \left[x_o + \varepsilon \cos\left(\omega t + \varphi\right) \right] m \omega^2 \\ f_{dy} &= \left[y_o + \varepsilon \sin\left(\omega t + \varphi\right) \right] m \omega^2 \end{aligned} \tag{3}$$

where ε denotes the mass eccentricity, and φ is the initial phase of the mass center.

The presence of these imbalance forces leads to a periodic runout during the rotation of the rotor which increases with the rotational speed squared. Unless $x_o = 0$ and/or $y_o = 0$, then there will also exist an electromagnetic imbalance in AMB which means that at this moment the electromagnetic center does not coincide with the geometric center. Fortunately, unlike conventional bearings, AMB provide a mean to handle this problem through proper control schemes.

III. Second-Order Sliding Mode

HOSM have emerged as a promising approach for handling the chattering problem while preserving the main advantages of the CSMC [18], [31], [32]. The high frequency oscillations could be significantly reduced since the actual discontinuous control action is acting on the higher time derivative of the sliding variable instead of the first time derivative as in CSMC [11], [33], [34]. It is considered an extension to the original sliding mode theory. In this context, CSMC are often referred to as first order sliding mode control (1-SMC). This section presents a brief review to the concepts of two popular 2-SMC, namely, the twisting and the suboptimal algorithms.

A. Problem Formulation

Consider the following nonlinear uncertain system:

$$\dot{x} = f\left(t, x\right) + g\left(t, x\right) u \tag{4}$$

where $x \in \mathbb{R}^n$ is the state vector, t is the time, $u \in \mathbb{R}$ is the control input, and $f\left(.\right)$, $g\left(.\right)$ are some smooth and uncertain vector functions.

Assume that a sliding variable σ is defined to fulfill the required control specifications as follows:

$$\sigma = \sigma\left(t, x\right) \tag{5}$$

and is deigned such that it has a relative degree r with respect to the control variable u. For 2-SMC, consider σ has a relative degree $r = 2$, and the second total time derivative of (5) can be formulated as:

$$\ddot{\sigma} = \alpha\left(t, x\right) + \beta\left(t, x\right) u \tag{6}$$

where $\alpha\left(.\right)$, $\beta\left(.\right)$ are uncertain and smooth functions and only their bounds σ_0, Γ_m, Γ_M, and Φ are known and fulfill the following inequalities [11]:

$$0 < \Gamma_m \le \beta \le \Gamma_M, \quad \left|\alpha\right| \le \Phi, \quad \left|\sigma\right| < \sigma_0 \tag{7}$$

The control objective in 1-SMC is to drive the sliding variable σ to zero in finite time, while for 2-SMC, it is required to drive both the sliding variable σ and it time derivative $\dot{\sigma}$ to zero in finite time. This is done by means of a discontinuous control action which acts on the second derivative of the sliding variable $\ddot{\sigma}$ [33]. In the following subsections, two 2-SMC algorithms that fulfill this control objective are presented.

B. Twisting Algorithm

Historically, the twisting algorithm is considered the first developed technique that falls under the category of 2-SMC algorithms. This algorithm depends on the switching between two different control gains such that the state trajectory is steered in a spiral (twisting) manner to converge in finite time to the origin, see Fig. 2 (a). This control algorithm can be defined as follows [31]:

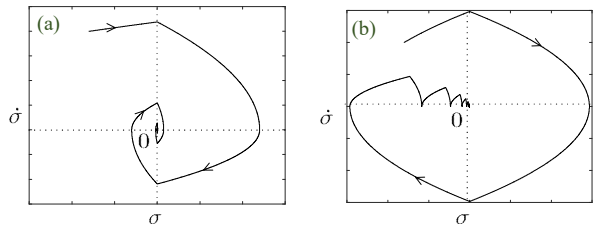

Fig. 2. Phase trajectory for 2-SMC: (a) twisting algorithm, (b) suboptimal algorithm (for a double integrator system).

$$\upsilon_{twist}(t)=\begin{cases}-\rho_t\,\mathrm{sgn}(\sigma), & if\ \sigma\dot{\sigma}\le 0\\ -\rho_T\,\mathrm{sgn}(\sigma), & if\ \sigma\dot{\sigma}>0\end{cases} \tag{8}$$

Appropriate values for ρ_t and ρ_T have to be chosen in order to guarantee that the trajectory twisting around the origin of the $\sigma\dot{\sigma}$ plane in finite time. The corresponding sufficient conditions to achieve this task are given as follows [31]:

$$\begin{aligned}&\rho_T>\rho_t,\ \rho_t>\frac{4\Gamma_M}{\sigma_0},\ \rho_t>\frac{\Phi}{\Gamma_m},\ \text{and}\\ &\Gamma_m\rho_T-\Phi>\Gamma_M\rho_t+\Phi\end{aligned} \tag{9}$$

C. Suboptimal Algorithm

The bang-bang controller is a classical time optimal control law characterized by switching between two extreme bounds. It is one of many options proposed in the literature for stabilizing uncertain nonlinear second systems in finite time. However, the application of this optimal controller requires a complete information about the states of the system. The problem of the finite time stabilization of uncertain second order nonlinear systems with incomplete state measurements was addressed in [35] in which the suboptimal algorithm, inspired by the classical time optimal bang-bang control of a double integrator, was derived using a sub-time-optimal feedback to fulfill this objective. Unlike the twisting algorithm which makes the trajectories converges non-monotonically in finite time to the origin of the $\sigma\dot{\sigma}$ phase plane, this algorithm yields a monotonic convergence. Moreover, the driven trajectories show twisting and jumping behaviors while converging to the origin, see Fig. 2 (b). This algorithm can be defined as follows [33], [35]:

$$\upsilon_{sub}=\begin{cases}\eta_{sub}\,\rho_{sub}\,\mathrm{sgn}\left(\sigma(t)-0.5\,\sigma_M(t)\right) & if\ \varpi>0\\ \rho_{sub}\,\mathrm{sgn}\left(\sigma(t)-0.5\,\sigma_M(t)\right) & if\ \varpi\le 0\end{cases} \tag{10}$$

where $\varpi=\left[\sigma(t)-0.5\,\sigma_M(t)\right]\left[\sigma_M(t)-\sigma(t)\right]$, η_{sub} and ρ_{sub} are positive control variables, σ_M is the value of σ recorded when $\dot{\sigma}$ was detected equal to zero at the last time. σ_M is initialized to zero and then updated by inspecting the last recorded value of σ. The practical implementation of this algorithm requires the online estimation of σ_M which can be simply realized by checking the sign change of the difference $\Delta\sigma$ between the successive measurements of σ [11]. Thus, σ_M can be estimated as:

$$\begin{aligned}&\sigma_M(t)=\begin{cases}\sigma(0), & 0\le t<t_{M_1}\\ \sigma\left(t_{M_i}\right), & t_{M_i}\le t<t_{M_{i+1}}\end{cases}\\ &i=1,2,....\end{aligned} \tag{11}$$

where t_{M_i} are the time instants at which $\dot{\sigma}$ was detected equal to zero. To guarantee a finite time convergence, the control parameters can be tuned according to the following inequalities [33]:

$$\begin{cases}\eta_{sub}\in(0,1]\cap\left(0,\dfrac{3\Gamma_m}{\Gamma_M}\right)\\ \rho_{sub}>\max\left(\dfrac{\Phi}{\eta_{sub}\,\Gamma_m},\dfrac{4\Phi}{3\Gamma_m-\eta_{sub}\Gamma_M}\right)\end{cases} \tag{12}$$

The above constraints represent the sufficient conditions.

IV. Control Design

A. Control Objective

For the sake of simplifying the control design process, a simple second-order model for one controlled axis in terms of the position tracking error $\tilde{q}=q_r-q$ can be formulated where q_r represents the position reference while q is the measured position signal (e.g. $q = y_1$ for the vertical axis at bearing B_1). It can be shown that this simplified model is described by:

$$\begin{aligned}&\dot{\tilde{q}}_1=\tilde{q}_2\\ &\dot{\tilde{q}}_2=a\,\tilde{q}_1-b\,u-d\end{aligned} \tag{13}$$

where $\tilde{q}_1=\tilde{q}$ and $\tilde{q}_2=\dot{\tilde{q}}$, u is the control input, a and b are the system parameters, and $d(t)$ represents the lumped external disturbances to the system which is assumed to be unknown but bounded. The state space model (13) can be re-written in a compact form as:

$$\dot{\underline{q}}=f+g\,u+w \tag{14}$$

where $\underline{q}=\begin{bmatrix}\tilde{q}_1\\ \tilde{q}_2\end{bmatrix}$, $f=\begin{bmatrix}0 & 1\\ a & 0\end{bmatrix}$, $g=\begin{bmatrix}0\\ -b\end{bmatrix}$, and $w=\begin{bmatrix}0\\ -d\end{bmatrix}$.

Again, the control objective is the stabilization and regulation of the rotor around the equilibrium point in the presence of external harmonic disturbances. Since the external disturbances are time varying, it could be infeasible to achieve a complete disturbance rejection using a feedback controller [36]. Instead, the control objective is to achieve a disturbance

attenuation throughout a wide range of rotational speeds.

The proposed control schemes based on 2-SMC concepts are composed of two components. The first component is a linear controller while the second component exploits the 2-SMC concepts which can be considered as an add-on to the stabilizing linear controller. A PID is selected to represent the linear controller and this control component is common to all the proposed schemes.

B. Twisting 2-SMC

Consider the sliding variable is defined as follows

$$\sigma = \tilde{q}_2 + \lambda_t \tilde{q}_1 \tag{15}$$

where λ_t is a positive constant. The proposed controller (PID-TWIST) can be defined as follows:

$$u_{PID-TWIST} = k_p \tilde{q}_1 + k_d \tilde{q}_2 + k_i \int_0^t \tilde{q}_1 \, d\tau - \int_0^t \upsilon_{twist} \, d\tau \tag{16}$$

It should be noted that the system (13) has a relative degree r = 1 with respect to the chosen output function (15). Furthermore, the proposed twisting controller is "hidden" under an integral action to alleviate the chattering effect introduced by the discontinuous action. Therefore, the discontinuous component acts on the second derivative of the sliding variable instead of the first derivative as in the 1-SMC. This can be illustrated by deriving the first and second derivatives of the sliding variable (15) respectively as follows:

$$\begin{aligned} \dot{\sigma} &= \frac{\partial \sigma}{\partial \underline{q}} . \frac{\partial \underline{q}}{\partial t} \\ &= \frac{\partial \sigma}{\partial \underline{q}} \left[f + g \, u_{PID-TWIST} + w \right] \end{aligned} \tag{17}$$

$$\begin{aligned} \ddot{\sigma} &= \frac{\partial \dot{\sigma}}{\partial \underline{q}} \left[f + g \, u_{PID-TWIST} + w \right] + \frac{\partial \dot{\sigma}}{\partial u_{PID-TWIST}} \dot{u}_{PID-TWIST} \\ &= \underbrace{\frac{\partial \dot{\sigma}}{\partial \underline{q}} \left[f + g \, u_{PID-TWIST} + w \right] + \frac{\partial \dot{\sigma}}{\partial u_l} \dot{u}_l}_{\phi_t} - \underbrace{\frac{\partial \dot{\sigma}}{\partial \upsilon_{twist}}}_{\gamma_t} \upsilon_{twist} \\ &= \phi_t - \gamma_t \, \upsilon_{twist} \end{aligned} \tag{18}$$

where u_l is the linear controller comprising the PID control action of (16).

C. Suboptimal 2-SMC

From (11), it is noticed that the successful implementation of the suboptimal algorithm depends on the accuracy of estimating σ_M. Thus, the performance of this algorithm could be affected by the presence of measurement noise if a simple numerical differentiator is employed. As a mitigation to this problem, we propose replacing the numerical differentiator by a high gain observer (HGO) for the sake of estimating σ_M and $\dot{\sigma}$ from σ. Furthermore, the HGO is also used as a replacement to the derivative action component in the PID controller. Besides the desire to reduce the effect of measurement noise, the HGO is selected because of its simplicity. In this section, we present the development of two control schemes based on the concepts of the suboptimal 2-SMC. The first one employs the simple numerical differentiator while the second one relies on the HGO.

The design process of both the suboptimal-based controllers also comprises two steps. Consider first, the sliding variable chosen as follows[1]:

$$\sigma = \tilde{q}_1 \tag{19}$$

It is noticed that the system (13) has a relative degree r = 2 with respect to the chosen output function (19). The two controllers are described below.

1) The First Control Scheme

The first suboptimal-based controller (PID-SUB1) can be defined as follows:

$$u_{PID-SUB1} = k_p \tilde{q}_1 + k_d \tilde{q}_2 + k_i \int_0^t \tilde{q}_1 \, d\tau - \upsilon_{sub} \tag{20}$$

The discontinuous component acts directly on the second derivative of the sliding variable instead of the first derivative as in the 1-SMC. This can be illustrated by deriving the second derivative of the sliding variable as follows:

$$\begin{aligned} \ddot{\sigma} &= \underbrace{\left(a - b k_p\right) \tilde{q}_1 - b k_d \tilde{q}_2 - b k_i \int_0^t \tilde{q}_1 \, d\tau + d}_{\phi_{sub}} \underbrace{\pm b}_{\gamma_{sub}} \upsilon_{sub} \\ &= \phi_{sub} + \gamma_{sub} \, \upsilon_{sub} \end{aligned} \tag{21}$$

2) The Second Control Scheme

If the measured output signal is q_1 and it is required to estimate its time-derivative q_2, then the HGO can be defined as [36]:

$$\begin{aligned} \dot{q}_1^* &= q_2^* + \frac{\alpha_1}{\varepsilon} \left(q_1 - q_1^* \right) \\ \dot{q}_2^* &= \frac{\alpha_2}{\varepsilon} \left(q_1 - q_1^* \right) \end{aligned} \tag{22}$$

where ε, α_1 and α_2 are positive constants with $\varepsilon \ll 1$, and q_1^* and q_2^* represent the estimated signals of q_1 and q_2 respectively. Incorporating the HGO with the suboptimal algorithm, the second proposed suboptimal controller (PID-SUB2) controller can be formulated as:

$$u_{PID-SUB2} = k_p \tilde{q}_1^* + k_d \tilde{q}_2^* + k_i \int_0^t \tilde{q}_1^* \, d\tau - \upsilon_{sub} \tag{23}$$

[1] A suboptimal controller based on a PD-like sliding variable was also considered but the experimental results of this controller was inferior compared to the linear controller. Therefore, we decided to remove this part for brevity and present the version that yields a good performance.

where $\tilde{q}_1^* = q_r - q_1^*$ is the tracking error while $\tilde{q}_2^*$ is its time derivative.

D. Remark on the Stability of 2-SMC Algorithms

It is common to use the Lyapunov approach to address the stability, robustness and convergence rate to the equilibrium point for 1-SMC. However, a similar treatment is not usually applicable to HOSM. Instead, either geometric-based techniques such as majorant curves or homogeneity are often employed to proof the convergence to the origin of the $\sigma\dot{\sigma}$ phase plane. Detailed stability proofs for the 2-SMC algorithms presented in this paper can be found in [11].

V. Simulation and Experimental Results

A. AMB Setup

Fig. 3 shows a photo of the AMB test rig. The experimental setup is composed of a shaft for which the driven terminal is supported by a mechanical ball bearing while the non-driven terminal is supported by a radial permanent magnet-biased active magnetic bearing (PM-AMB). The magnetic bearing has an air gap of 1.0 mm and is protected by a safety bearing with a 0.5 mm clearance. An induction motor is used for rotating the shaft up to 3000 revolution-per-minute (RPM). Two position sensors of inductive type are used for position control, and two current sensors are also required for closing the current control loop. Two single phase inverter circuits (one for each axis) are used to amplify the control current. Digital PI controllers are implemented on the digital signal processing (DSP) board for regulating the currents in the power amplifier loops.

B. Implementation Issues

Since the proposed control schemes are explicitly composed of two control actions, the implementation and tuning process can be split into two phases. The first phase considers the realization of the PID controller to stabilize the inherently unstable plant. There exist many techniques proposed in the literature for tuning PID control in general [37] and for AMB systems in particular, e.g. [1], [38]. In this work, the PID gains were initially selected via computer-aided simulation and then finely tuned after extensive experimentations. The second phase of tuning process is devoted to the 2-SMC algorithms. As illustrated in Section III, the twisting and the suboptimal algorithms can be tuned according to (9) and (12) respectively. However, it should be indicated that these conditions are only sufficient but not necessary. Furthermore, they are very conservative since they are based on the worst-case estimate of the controlled plant bounds and applying them could result in very large control signals. Therefore, it is usually advised to tune 2-SMC algorithms heuristically via numerical simulations [11].

To facilitate the computer-aided tuning process for the proposed 2-SMC algorithms, we present some guidelines in the following sentences. For the twisting algorithm, there are three parameters to be tuned. At first, a set of values for tuning parameter λ_t is arbitrarily selected. Then λ_t is initially adjusted to the minimal element. The other two parameters ρ_T and ρ_t are then interactively tuned to attain as high disturbance attenuation as possible while satisfying the condition $\rho_T > \rho_t$. Since the objective is to attenuate harmonic disturbances in a wide speed range, the controller is tuned and tested against the worst-case condition. For our system, the worst-case in terms of vibration levels corresponds to the critical speed encountered at 2600 RPM when PID control only is applied to the system. The above procedure is repeated for each member of λ_t set values. Finally, the group that achieves the best disturbance attenuation throughout the entire speed range is chosen as design setting for the proposed algorithm. A similar approach can be adopted for selecting the parameters of the suboptimal algorithm. For tuning the HGO, [36] can be consulted. Once, the proposed schemes are tuned with numerical simulations, they are then finely tuned with experimentation. The final settings are provided in Table III, see Appendix I. It should be emphasized that the same PID controller is common to all the control schemes.

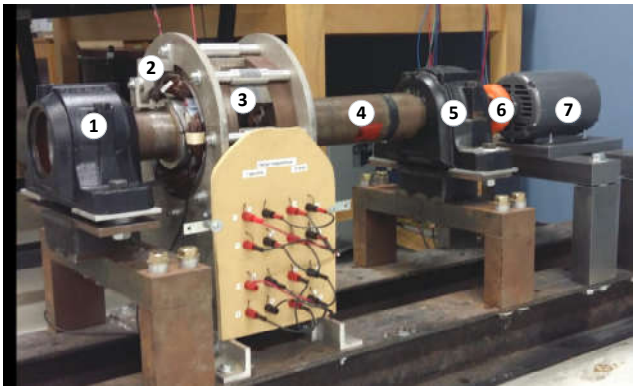

Fig. 3. radial magnetic bearing test rig: (1) safety bearing, (2) position sensor, (3) PM-AMB, (4) shaft, (5) ball bearing, (6) flexible

The configuration of the proposed schemes is shown in Fig. 4. The control algorithms were realized using the Spectrum Digital eZdsp F2812 board. The board employs TMS320F2812 DSP which is a 32-bit DSP with fixed-point arithmetic and includes six dual pulse width modulation (PWM) channels and 16 12-bit analog-to-digital converters (ADCs). A sampling rate of 10 kHz was used for executing the control algorithms.

C. Simulation Results

In this subsection, a comparative analysis via numerical simulation is carried out between a well-tuned PID controller and the proposed 2-SMC schemes to demonstrate the effectiveness and the superiority of the proposed techniques in handling time-varying harmonic disturbances. To ensure a fair comparison, the proposed schemes employs the same PID controller but equipped with the 2-SMC components as add-ons. To fulfill this objective, the rotor-AMB model (1) described in Section II was implemented in the environment of MATLAB/Simulink. Furthermore, the effect of the rotor mass imbalance forces acting throughout a wide speed range are represented by (3). For the sake of simplicity, we neglected the electromagnetic imbalance (i.e. $x_o = 0$ and $y_o = 0$) and also assumed that the harmonic disturbances have a constant amplitude ($\varepsilon m = 30\ N$) while their frequency initially starts at

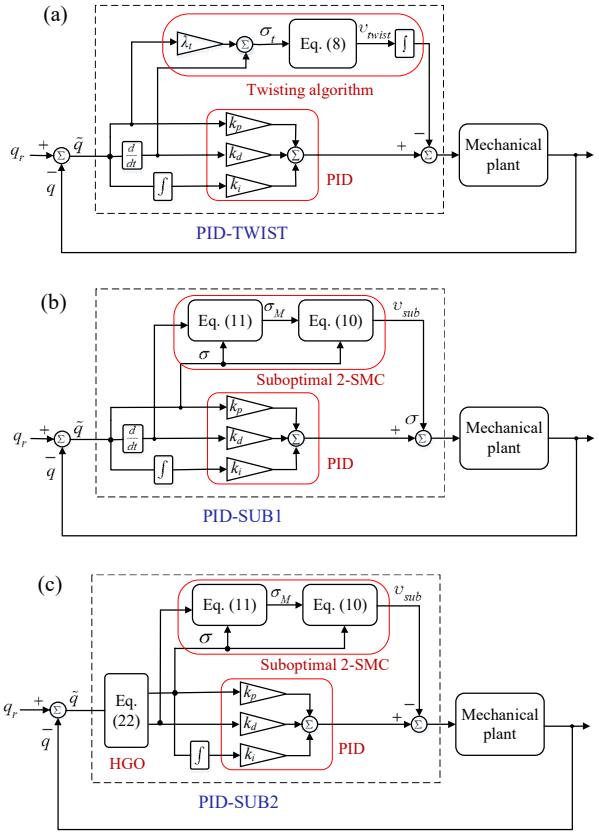

Fig. 4. The configuration of the proposed second sliding mode control schemes: (a) PID-TWIST, (b) PID-SUB1, and (c) PID-SUB2.

0.1 Hz and linearly increases up to 50 Hz in 10 s. Moreover, a white-noise is injected to the feedback loop to emulate the behavior of a noisy measurement system.

Fig. 5 shows a comparative simulation results of the proposed controllers against PID controller for the vertical axis in terms of attenuating the time-varying harmonic disturbance. For the PID case, one can notice that the harmonic disturbances make the vertical position deviates from the origin. Furthermore, this deviation increases with the rotational speed until it reaches a peak value around 2000 RPM. This amplification in the position deviation is due to the coincidence between the operating speed and a natural frequency of the PID-controlled system. It is also remarkable that the peak to peak displacement reduces from 92.38 μm in the PID case to 70.49 μm, 52.55 μm, and 41.39 μm for the PID-SUB1, PID-SUB2, and PID-TWIST cases respectively. In other words, adopting the proposed PID-SUB1, PID-SUB2, and PID-TWIST compensation techniques respectively yields 23.7%, 43.12%, and 55.20% reduction in the peak to peak rotor displacements.

From these results, one can conclude that the twisting algorithm could achieve better disturbance attenuation to harmonic disturbances compared to the suboptimal algorithm. Furthermore, replacing the numerical differentiator with the HGO improves the performance in the presence of measurement noise. Moreover, the HGO can also be applied to the PID-TWIST algorithm for the sake of improving the

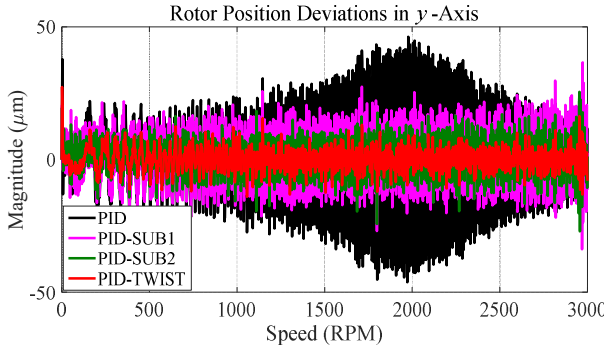

Fig. 5. Comparative simulation results of the proposed controllers against PID controller for attenuating a time-varying harmonic disturbance.

performance but on the price of increasing the complexity of the control scheme.

D. Experimental Validation of Proposed Methods

The proposed control schemes were experimentally implemented to demonstrate their effectiveness in attenuating time-varying harmonic disturbances. The rotor was driven up from standstill to 3000 RPM and the rotor displacements in the horizontal and vertical directions were recorded every 200 RPM rotational speed to examine the performance of the closed-loop system in the entire speed range. For the sake of evaluating the performance of the control schemes, the root-mean-square (RMS) and the maximum values of the recorded rotor displacements were calculated. These performance measures for all the control schemes are then plotted against rotational speeds to facilitate the comparative analysis, see Fig. 6 and 7. From Fig. 7, it is obvious that adopting a well-tuned PID controller alone yields non-uniform rotor deviations in the entire operating range with two peaks at 1400 RPM and 2600 RPM corresponding to the first two natural frequencies of the system. It is remarkable that these characteristics are not similar to simulation results presented in Fig. 5 which has one natural frequency at 2000 RPM. The reasons for this mismatch are mainly due to neglecting the fast dynamics (e.g. sensors and actuator) in the simulation analysis, the model parametric uncertainties, and applying constant amplitude time-varying harmonic disturbances.

On the other hand, one can observe that applying the proposed 2-SMC add-ons improves the performance and minimizes the deviations of the rotor, both in the horizontal and vertical directions because these add-ons which compensate the effect of the rotor mass imbalance forces. In other words, the introduction of the 2-SMC components to the PID-controlled plant results in increasing the effective stiffness of the AMB to the harmonic disturbances. From Fig. 6 and 7, it is noticed that the deviations of the rotor are almost uniform and effectively attenuated in the case of PID-TWIST controller although achieving a uniform stiffness throughout a wide-range of operating speeds is a nontrivial task since it is required to tune, simulate and test the performance of the algorithms at many speeds. Furthermore, the characteristics of the two suboptimal algorithms are comparable and slightly better than the PID control in the low speed range up to 2000 RPM. Beyond this rotation speed, the reduction in the PID-

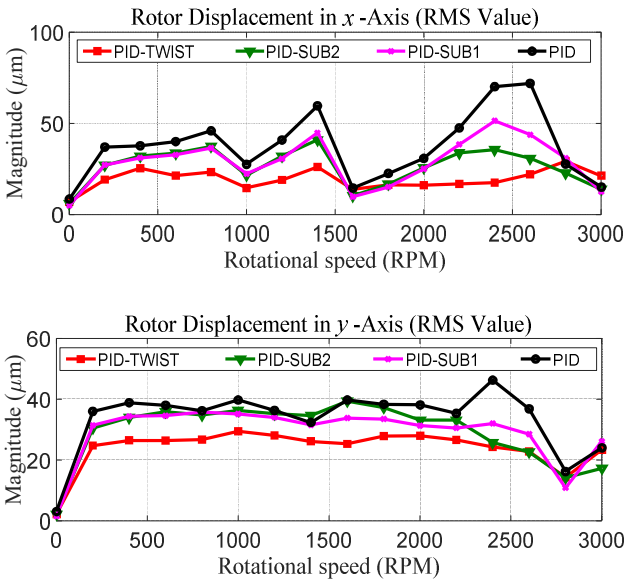

Fig. 6. Comparative experimental results for the RMS values of the horizontal and vertical rotor deviations up to 3000 RPM rotational speed.

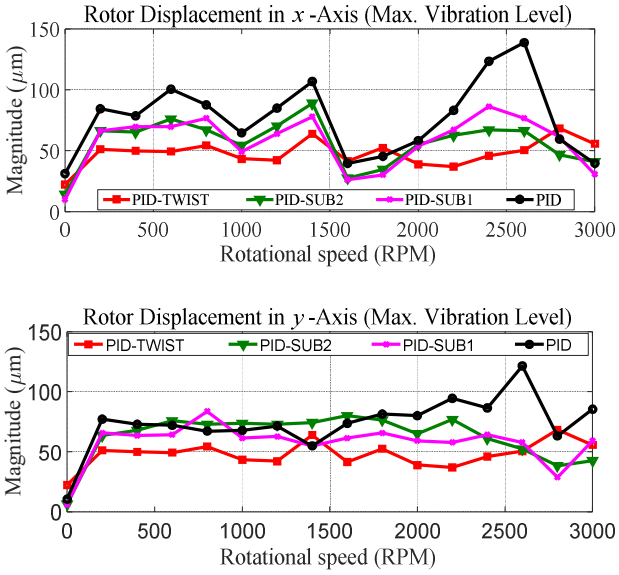

Fig. 7. Comparative experimental results for the maximum rotor deviations in the horizontal and vertical when rotated up to 3000 RPM.

SUB2 position deviations compared to the others is remarkable. The degraded performance of the PID-SUB1 algorithm at higher rotation speeds goes back to the inability of the simple numerical differentiator to estimate the signal σ_M properly due to the combined effect of measurement noise and the harmonic disturbances. In general, these remarks are compatible with the numerical simulation results.

To draw a conclusion on the performance of the control schemes in the entire speed range, the RMS performance measures are averaged. Furthermore, the maximum rotor position deviation encountered throughout the whole operating range is also picked and employed for fulfilling this objective. The averaged horizontal RMS rotor displacements, in the entire operating speed range, for PID-SUB1, PID-SUB2, and PID-TWIST are 30.15 μm, 27.58 μm, 20.13 μm, respectively against 39.26 μm for the PID controller which represent 23.2%, 29.75%, 48.73% reduction in the rotor position deviations from the geometric bearing center, respectively. The maximum horizontal rotor deviations, in the entire rotation range, for PID-SUB1, PID-SUB2, and PID-TWIST are 86.40 μm, 88.92 μm, 68.40 μm, respectively against 138.92 μm for the PID controller which represent 37.81%, 36.00%, 50.76% reduction in the rotor deviations, respectively. These performance measures for the horizontal and vertical directions are summed up in Table I.

VI. Conclusion

In this paper, three control algorithms based on the concepts of 2-SMC have been proposed to handle model uncertainties and time-varying harmonic disturbances in AMB systems operating in a wide range of rotor speeds. The first one relies on the twisting algorithm while the other two employ the suboptimal algorithm. Simulation and experiments were performed to validate the effectiveness of the proposed techniques. It was shown that the twisting and the suboptimal algorithms can attenuate the maximum rotor deviation by 50.76% and 37.81% respectively compared to the conventional linear controller. Furthermore, the proposed 2-SMC method is easy to apply in practice and requires no information about the rotational speed.

Appendix I

The main system parameters and control settings used in the simulations are respectively listed in Table II and Table III.

Appendix II

This appendix shows the limitation of applying the 2-SMC approach for handling harmonic disturbances. For instance, let us consider a 2-SMC technique when applied to (13) which represents the dynamics of one controlled axis of an AMB system and for the sake of simplifying the analysis let us neglect the chattering problem. The sliding variable can be selected as (15) and therefore its first and second time derivatives can be derived respectively as follows:

$$\dot{\sigma} = \dot{\tilde{q}}_2 + \lambda_t \tilde{q}_2 \tag{24}$$

$$\ddot{\sigma} = a\dot{\tilde{q}}_2 - b\ddot{u} - \dot{d} + \lambda_t \left[a\tilde{q}_1 - bu - d \right] \tag{25}$$

Let us assume that

Table I
A Summary for the Experimental Performance Measures

Control Scheme	Horizontal Axis		Vertical Axis	
	RMS (μm) (averaged)	MAX (μm)	RMS (μm) (averaged)	MAX (μm)
PID	39.26	138.92	35.50	121.50
PID-SUB1	30.15	86.40	30.90	83.70
PID-SUB2	27.58	88.92	30.92	80.10
PID-TWIST	20.13	68.40	25.40	62.10

Table II
Main Parameters of the PM-AMB Setup

Sym.	Description	Value	Unit
m	Rotor mass	61.5	kg
l	Rotor length	120	cm
D	Rotor diameter	90	mm
J_r	Rotor transverse moment of inertia	4.79	kg m^2
J_z	Rotor polar moment of inertia	0.086	kg m^2
k_s	PM-AMB Stiffness for x-axis and y-axis, respectively	28.05, 47.8	N/mm
k_i	PM-AMB current gain for x-axis and y-axis, respectively	609, 609	N/A
G	Nominal PM-AMB air-gap length	1	mm
G_{sb}	Nominal safety bearing clearance length	0.5	mm
R_c	Electromagnetic coil resistance	1.137	Ω
L_c	Electromagnetic coil inductance	0.136	H
V_{DC}	Dc voltage supply	30	V

Table III
Design Values for Controllers Coefficients

Algorithm	Design values
PID	$k_p = 3300$, $k_d = 10$, $k_i = 15000$
SUB1	$\rho_{sub} = 0.06$, $\eta_{sub} = 0.7$
SUB2	$\rho_{sub} = 0.13$, $\eta_{sub} = 0.5$, $\alpha_1 = 1$, $\alpha_2 = 3$, $\varepsilon = 0.001$
Twist	$\lambda_t = 100$, $\rho_t = 0.01$, $\rho_T = 0.07$.

$$\lambda_t = \sqrt{a} \tag{26}$$

It yields

$$\begin{aligned} \ddot{\sigma} &= -b\dot{u} - \dot{d} + \lambda_t \left[a\tilde{q}_1 - bu - d + \lambda_t \dot{\tilde{q}}_2 \right] \\ &= -b\dot{u} - \dot{d} + \lambda_t \dot{\sigma} \end{aligned} \tag{27}$$

then the equivalent control action u_{eq} can be derived as follows:

$$\ddot{\sigma} = \dot{\sigma} = \sigma = 0 \rightarrow \dot{u}_{eq} = -\frac{\dot{d}}{b} \tag{28}$$

If the external disturbance is sinusoidal and similar to (3):

$$d = \varepsilon m \omega^2 \cos(\omega t) \tag{29}$$

then its time derivative would be

$$\dot{d} = -\varepsilon m \omega^3 \sin(\omega t) \tag{30}$$

Therefore (28) can be formulated as:

$$\dot{u}_{eq} = b^{-1} \varepsilon m \omega^3 \sin(\omega t) \tag{31}$$

Consider that the electrical dynamics of the system are described by the following first-order system [1]:

$$\frac{du}{dt} = \frac{V}{L} - \frac{R}{L} u \tag{32}$$

where V is applied voltage, R and L are the total resistance and inductance of one controlled winding respectively, while u represents the control current. If the resistance of the electromagnetic coil is neglected for simplicity, the maximum slew-rate should satisfy the following condition:

$$\left| \frac{du}{dt} \right| \le \frac{V_{\max}}{L} \tag{33}$$

From (28) and (33), the external disturbances can be effectively handled according to the following condition:

$$\dot{d} \le \frac{b V_{\max}}{L} \tag{34}$$

Therefore, the angular frequency of the sinusoidal disturbance should satisfy the following relationship:

$$\omega \le \sqrt[3]{\frac{b}{\varepsilon m L} V_{\max}} \tag{35}$$

One can conclude that the application of a 2-SMC technique to handle harmonic disturbances is feasible as long as the above condition is satisfied.

REFERENCES

[1] H. Bleuler *et al.*, *Magnetic Bearings: Theory, Design, and Application to Rotating Machinery*. Berlin, Heidelberg: Springer Berlin Heidelberg, 2009.

[2] M. Fujita, K. Hatake, and F. Matsumura, "Loop shaping based robust control of a magnetic bearing," *IEEE Control Syst.*, vol. 13, no. 4, pp. 57–65, Aug. 1993.

[3] A. Noshadi, J. Shi, W. S. Lee, P. Shi, and A. Kalam, "System Identification and Robust Control of Multi-Input Multi-Output Active Magnetic Bearing Systems," *IEEE Trans. Control Syst. Technol.*, pp. 1–13, 2015.

[4] H. M. N. K. Balini, J. Witte, and C. W. Scherer, "Synthesis and implementation of gain-scheduling and LPV controllers for an AMB system," *Automatica*, vol. 48, no. 3, pp. 521–527, Mar. 2012.

[5] B. Lu, H. Choi, G. D. Buckner, and K. Tammi, "Linear parameter-varying techniques for control of a magnetic bearing system," *Control Eng. Pract.*, vol. 16, no. 10, pp. 1161–1172, Oct. 2008.

[6] J. Kejian, Z. Changsheng, and C. Liangliang, "Unbalance Compensation by Recursive Seeking Unbalance Mass Position in Active Magnetic Bearing-Rotor System," *IEEE Trans. Ind. Electron.*, vol. 62, no. 9, pp. 5655–5664, Sep. 2015.

[7] Q. Chen, G. Liu, and S. Zheng, "Suppression of imbalance vibration for AMBs controlled driveline system using double-loop structure," *J. Sound Vib.*, vol. 337, pp. 1–13, Feb. 2015.

[8] Chao Bi, Dezheng Wu, Quan Jiang, and Zhejie Liu, "Automatic learning control for unbalance compensation in active magnetic bearings," *IEEE Trans. Magn.*, vol. 41, no. 7, pp. 2270–2280, Jul. 2005.

[9] J. J. E. Slotine and W. A. LI, *Applied Nonlinear Control*. Prentice Hall, 1991.

[10] K. D. Young, V. I. Utkin, and U. Ozguner, "A control engineer's guide to sliding mode control," *IEEE Trans. Control Syst. Technol.*, vol. 7, no. 3, pp. 328–342, May 1999.

[11] Y. Shtessel, C. Edwards, L. Fridman, and A. Levant, *Sliding Mode Control and Observation*. New York, NY: Springer New York, 2014.

[12] A. Charara, J. De Miras, and B. Caron, "Nonlinear control of a magnetic levitation system without premagnetization," *IEEE Trans. Control Syst. Technol.*, vol. 4, no. 5, pp. 513–523, 1996.

[13] Shyh-Leh Chen, Sung-Hua Chen, and Shi-Teng Yan, "Experimental validation of a current-controlled three-pole magnetic rotor-bearing system," *IEEE Trans. Magn.*, vol. 41, no. 1, pp. 99–112, Jan. 2005.

[14] Y. Fan, C. Y. Christian, Y. Lee, and C. Lin, "Design of a Variable Structure Controller Based on the Force Estimator for a Single Active Magnetic Bearings Suspended Rotor System," in *Proc. of the 13th International Symposium on Magnetic Bearings (ISMB13)*, 2012.

[15] F.-J. Lin, S.-Y. Chen, and M.-S. Huang, "Intelligent double integral sliding-mode control for five-degree-of-freedom active magnetic bearing system," *IET Control Theory Appl.*, vol. 5, no. 11, pp. 1287–1303, Jul. 2011.

[16] S. Sivrioglu and K. Nonami, "Sliding mode control with time-varying hyperplane for AMB systems," *IEEE/ASME Trans. Mechatronics*, vol. 3, no. 1, pp. 51–59, 1998.

[17] Y. XU and K. NONAMI, "A Fuzzy Modeling of Active Magnetic Bearing System and Sliding Mode Control with Robust Hyperplane Using .MU.-Synthesis Theory," *JSME Int. J. Ser. C*, vol. 46, no. 2, pp. 409–415, 2003.

[18] A. Levant, "Higher-order sliding modes, differentiation and output-

feedback control," *Int. J. Control*, vol. 76, no. 9–10, pp. 924–941, Jan. 2003.
[19] A. Levant, "Principles of 2-sliding mode design," *Automatica*, vol. 43, no. 4, pp. 576–586, Apr. 2007.
[20] M. Reichhartinger and M. Horn, "Application of higher order sliding-mode concepts to a throttle actuator for gasoline engines," *IEEE Trans. Ind. Electron.*, vol. 56, no. 9, pp. 3322–3329, 2009.
[21] A. Pisano, A. Davila, L. Fridman, and E. Usai, "Cascade Control of PM DC Drives Via Second-Order Sliding-Mode Technique," *IEEE Trans. Ind. Electron.*, vol. 55, no. 11, pp. 3846–3854, Nov. 2008.
[22] A. Damiano, G. L. Gatto, I. Marongiu, and A. Pisano, "Second-Order Sliding-Mode Control of DC Drives," *IEEE Trans. Ind. Electron.*, vol. 51, no. 2, pp. 364–373, Apr. 2004.
[23] B. Beltran, T. Ahmed-Ali, and M. Benbouzid, "High-Order Sliding-Mode Control of Variable-Speed Wind Turbines," *IEEE Trans. Ind. Electron.*, vol. 56, no. 9, pp. 3314–3321, Sep. 2009.
[24] J. Rivera Dominguez, C. Mora-Soto, S. Ortega-Cisneros, J. J. Raygoza Panduro, and A. G. Loukianov, "Copper and Core Loss Minimization for Induction Motors Using High-Order Sliding-Mode Control," *IEEE Trans. Ind. Electron.*, vol. 59, no. 7, pp. 2877–2889, Jul. 2012.
[25] M. Defoort, F. Nollet, T. Floquet, and W. Perruquetti, "A Third-Order Sliding-Mode Controller for a Stepper Motor," *IEEE Trans. Ind. Electron.*, vol. 56, no. 9, pp. 3337–3346, Sep. 2009.
[26] M. S. Kandil, P. Micheau, J. P. Trovao, L. S. Bakay, and M. R. Dubois, "Hybrid Magnetic Bearing Regulation via Super Twisting Control," in *2015 15th International Conference on Control, Automation and Systems (ICCAS)*, 2015, pp. 1566–1571.
[27] V. V. H. and B. D. Hoang, "Second Order Sliding Mode Control Design for Active Magnetic Bearing System," in *AETA 2015: Recent Advances in Electrical Engineering and Related Sciences. Lecture Notes in Electrical Engineering*, vol. 371, V. H. Duy, T. T. Dao, I. Zelinka, H.-S. Choi, and M. Chadli, Eds. Cham: Springer International Publishing, 2016.
[28] S.-Y. Chen and F.-J. Lin, "Robust Nonsingular Terminal Sliding-Mode Control for Nonlinear Magnetic Bearing System," *IEEE Trans. Control Syst. Technol.*, vol. 19, no. 3, pp. 636–643, May 2011.
[29] H.-K. Chiang, C.-C. Fang, W.-B. Lin, and G.-W. Chen, "Second-order sliding mode control for a magnetic levitation system," *2011 8th Asian Control Conf.*, pp. 602–607, 2011.
[30] S. Jain, J. P. Mishra, and D. B. Talange, "A robust control approach for magnetic levitation system based on super-twisting algorithm," in *2015 10th Asian Control Conference (ASCC)*, 2015, vol. 7, pp. 1–6.
[31] A. LEVANT, "Sliding order and sliding accuracy in sliding mode control," *Int. J. Control*, vol. 58, no. 6, pp. 1247–1263, Dec. 1993.
[32] S. V. Emel'yanov, S. K. Korovin, and A. Levant, "High-order sliding modes in control systems," *Comput. Math. Model.*, vol. 7, no. 3, pp. 294–318, 1996.
[33] G. Bartolini, A. Ferrara, A. Levant, and E. Usai, "On second order sliding mode controllers," in *Variable structure systems, sliding mode and nonlinear control*, London: Springer London, 1999, pp. 329–350.
[34] G. Bartolini, A. Pisano, E. Punta, and E. Usai, "A survey of applications of second-order sliding mode control to mechanical systems," *Int. J. Control*, vol. 76, no. 9–10, pp. 875–892, Jan. 2003.
[35] G. Bartolini, A. Ferrara, and E. Usai, "Applications of a sub-optimal discontinuous control algorithm for uncertain second order systems," *Int. J. Robust Nonlinear Control*, vol. 7, no. 4, pp. 299–319, Apr. 1997.
[36] H. K. Khalil, *Nonlinear Systems*. Prentice Hall PTR, 2002.
[37] A. Visioli, *Practical PID Control*, 1st ed. Springer London, 2006.
[38] P. Anantachaisilp and Z. Lin, "An experimental study on PID tuning methods for active magnetic bearing systems," *Int. J. Adv. Mechatron. Syst.*, vol. 5, no. 2, p. 146, 2013.

Mohamed S. Kandil (S'14) obtained his B.Sc. and M.Sc. degrees in Electrical Engineering from Zagazig University, Egypt in 2007 and 2011, respectively. He received a Ph.D. degree in Electrical Engineering from University of Sherbrooke, Canada in 2016. Between 2007 and 2008, he worked in industry as a design engineer. Between 2008 and 2012, he was a Lecturer assistant with the department of power systems and electric machines, Zagazig University, Egypt. In 2012, he joined the Department of Electrical Engineering and Computer Engineering, University of Sherbrooke, Sherbrooke, QC, Canada, as a research and teaching assistant. His current research interests include magnetic levitation systems and nonlinear and adaptive control techniques applied to mechatronics, automotive systems, and renewable energies.

Maxime R. Dubois (M'99) obtained his B.Sc. in Electrical Engineering from the Université Laval, Québec, Canada in 1991. He received a Ph.D. cum laude from Delft University of Technology in The Netherlands in 2004. Between 2004 and 2011, he has been with the Université Laval. Since 2011, Prof. Dubois has been Associate Professor at University of Sherbrooke, Canada. He is the founder of Eocycle Technologies Inc., a company specialized in the development of TFPM. He is also the founding professor of the company AddEnergie Technologies. His fields of interest are electrical machines and power electronics applied to the field of wind energy, energy storage and electric vehicles. He was the Technical Program Committee Chair of the 2015 IEEE Vehicle Power and Propulsion Conference and a Guest Editor for the Special Issue of IET Electrical Systems in Transportation on Design, Modeling and Control of electric Vehicles.

Loicq S. Bakay was born in Kousseri, Cameroon, in 1978. He obtained his Masters of Science in Electrical Engineering from Swiss Federal Institute of Technology (EPFL), Lausanne, Switzerland in 2007. He received a Ph.D. from the Université Laval, Québec, Canada in 2012. Between 2010 and 2011 he worked at OPAL-Real Time technologies as a power electronic researcher Engineer. Since 2011, Dr. Bakay has been working for General Electric (GE) as Lead Tendering Engineer. His fields of interest are electrical machines and auxiliaries, and power electronics applied to renewable energies.

João Pedro F. Trovão (S'08 - M'13) was born in Coimbra, Portugal, in 1975. He received the M.Sc. degree and the Ph.D. degree in Electrical Engineering from the University of Coimbra, Coimbra, Portugal, in 2004 and 2013, respectively. From 2000 to 2014, he was a Teaching Assistant and an Assistant Professor with the Polytechnic Institute of Coimbra–Coimbra Institute of Engineering (IPC–ISEC), Portugal. Since 2014, he has been a Professor with the Department of Electrical Engineering and Computer Engineering, University of Sherbrooke, Sherbrooke, QC, Canada, where he holds the Canadian Research Chair position in Efficient Electric Vehicles with Hybridized Energy Storage Systems. His research interests cover the areas of electric vehicles, hybridized energy storage systems, energy management and rotating electrical machines. J. P. F. Trovão was a Guest Editor for the Special Issue of IET Electrical Systems in Transportation on Energy Storage and Electric Power Sub-Systems for Advanced Vehicles. He is a Guest Editor for the Special Issue of IEEE Transactions on Vehicular Technology on Electric Powertrains for Future Vehicles.